Cause of kinematic differences during centrifugal and centripetal saccades

Ansgar R. Koene [*], Casper J. Erkelens

Department Physics of Man, Faculty of Physics and Astronomy, Utrecht University, Princetonplein 5, 3584 CC Utrecht, Netherlands

Abstract

Measurements of eye movements have shown that centrifugal movements (i.e. away from the primary position) have a lower maximum velocity and a longer duration than centripetal movements (i.e. toward the primary position) of the same size. In 1988 Pelisson proposed that these kinematic differences might be caused by differences in the neural command signals, oculomotor mechanics or a combination of the two.

By using the result of muscle force measurements that were made in recent years (Orbit[TM]1.8 Gaze mechanics simulation, Eidactics, San Francisco, 1999) we simulated the muscle forces during centrifugal and centripetal saccades. Based on these simulations we show that the cause of the kinematic differences between the centrifugal and centripetal saccades is the non-linear force–velocity relationship (i.e. muscle viscosity) of the muscles.

© 2002 Elsevier Science Ltd. All rights reserved.

Keywords: Saccade kinematics; Oculomotor plant; Centripetal; Centrifugal; Simulation

1. Introduction

Studies of saccade velocity profiles by Abel, Dell'Osso, Daroff, and Parker (1979), Collewijn, Erkelens, and Steinman (1988), Eggert, Mezger, Robinson, and Straube (1999), Pelisson and Prablanc (1988) and Rottach, Das, Wohlgemuth, Zivotofsky, and Leigh (1998) have shown that the kinematics of saccadic eye movements differ for movements towards the primary position (centripetal movements) and movements away from the primary position (centrifugal movements). In his 1988 paper Pelisson proposed that the observed kinematic differences might be caused either by the neural command signals or the oculomotor mechanics, or a combination of the two.

Regarding the neural command signals it has been known for many years (Robinson, 1964) that for a saccade to occur, a pulse-step signal must be sent from oculomotor nuclei to the extraocular muscles; a high frequency phasic activity (pulse) is required for the eyes to move quickly against high viscous forces and a regular

tonic activity (step) to hold the eyes at their new position against elastic restoring forces. The known anatomical connections between the pulse generator for horizontal saccades and the muscles suggest that the antagonistic pair of muscles is organized in a push–pull arrangement (see Fuchs, Kaneko, & Scudder, 1985). As a consequence, the phasic command would apparently produce opposite but proportional modulations of firing frequency in the agonist (pulse of activation, Fig. 1) and in the antagonist muscles (pulse of deactivation, Fig. 1). However electrophysiological recordings from motoneurons in monkey have shown that for saccade amplitudes larger then 10° antagonist motoneurons are totally inhibited irrespective of initial eye orientation (Cullen & Guitton, 1997; Fuchs & Lushei, 1970; Robinson, 1970). Therefore the intensity of the deactivation is equal to the tonic activity at the beginning of the saccade (Fig. 1). Since the tonic activity increases with the ocular deviation toward the muscle concerned, the deactivation of the antagonist muscle is proportional to the initial eye deviation in the opposite direction to the saccade (off direction). Thus the smaller the initial eye position in the off direction (i.e. the smaller the initial centripetal component) the smaller the deactivation step becomes. Pelisson and Prablanc argued that this loss of

---

[*] Corresponding author. Fax: +31-30-25-22-664.
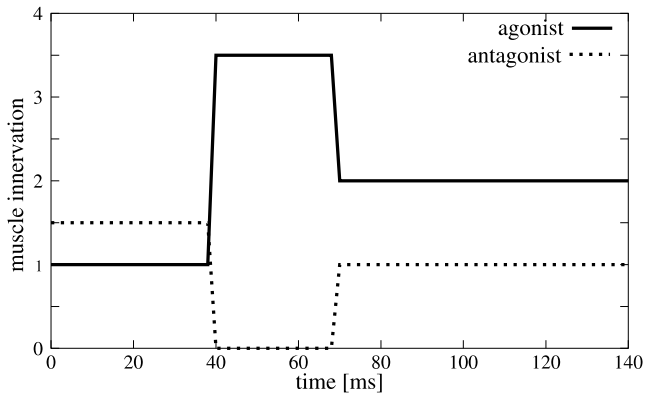*E-mail address:* a.koene@phys.uu.nl (A.R. Koene).

Fig. 1. Schematic representation of the pulse-step signal sent to the agonist and antagonist muscles.

signal between premotor burst neurons and motoneurons, related to the low tonic activity of the latter and proportional to initial eye position, is a reasonable explanation of the observed increase of maximum saccade velocity with initial centripetal component.

Pelisson and Prablanc went on to describe some of the mechanical non-linearities that have been found at the level of the ocular mechanics. In cat (Robinson, 1964) and in man (Collins, Lennerstrand, & Bach-Y-Rita, 1975a; Collins, O'Meara, & Scott, 1975b; Miller & Robinson, 1984; Miller, Pavlovski, & Shamaeva, 1999) extraocular muscles have non-linear length–tension relationships, with increased stiffness of the stretched (antagonist) muscle with ocular deviation. The viscous properties of the mechanical plant also seem non-linear (Collins et al., 1975a; Cook & Stark, 1968). They therefore felt that accurate simulations of the oculomotor plant are required to assess the effect of these mechanical non-linearities and of their complex interplay on the kinematics of saccades initiated from different initial positions.

Pelisson and Prablanc concluded that although the non-linearity of neural commands seems to be a reasonable explanation of the observed velocity changes, peripheral non-linearities cannot yet be ruled out.

In the 13 years since Collewijn et al. (1988) and Pelisson and Prablanc (1988) published their findings a great deal of work has been done on deriving better models of the oculomotor control system that drives saccades (Gancarz & Grossberg, 1998; Quaia, Lefevre, & Optican, 1999) and new data has allowed the construction of more detailed models of the ocular me-

chanics (Miller et al., 1999). The degree to which the difference in centrifugal and centripetal saccade kinematics is caused by neural signal saturation or eye plant mechanics, however, has as yet remained unanswered.

Answering this question may help us to gain more insight into the way in which the signal driving the saccades is modulated to account for starting position differences.

In this paper we investigate the degree to which the mechanical and the neural non-linearities contribute to the kinematic differences between centrifugal and centripetal saccades. Based on the velocity profiles of centrifugal and centripetal saccades we calculate the forces and muscle innervations during these eye movements. For the calculation of the forces in the muscles, and the corresponding muscle innervations, we used a model of the eye plant based on the work by Clark and Stark (1974a,b), Collins et al. (1975a), Pfann, Keller, and Miller (1995) and Robinson and Zuber (1981) and the data from implanted force transducer experiments published by Miller and Robins (1992), Miller et al. (1999) and Pfann et al. (1995). In contrast to these earlier studies, however, we did not use the model to synthesize eye movements from muscle innervation profiles. Instead we inverted the model to allow us to calculate the muscle innervations and muscle forces from eye movement profiles. An overview of the step-wise process of calculating the muscle forces and innervation during saccades is shown in Fig. 2. At each step we compared the force (innervation) profiles that were calculated for the centrifugal saccade with the corresponding profiles for the centripetal saccade and correlate this with the kinematic differences.

2. Method

In order to determine the contributions of the mechanical and neural properties of the saccade system to the kinematic differences between centrifugal and centripetal saccades we measured the eye movements and used a model of the eye plant, based on implanted force transducer data from Miller et al. (1999), to simulate the forces acting on the eye during these saccades.

The total force acting on the eye (F_{total}) was found by taking the second derivative of the measured eye position profiles (resulting in eye acceleration profiles) and applying Newton's third law. The passive forces ($F_{passive}$),
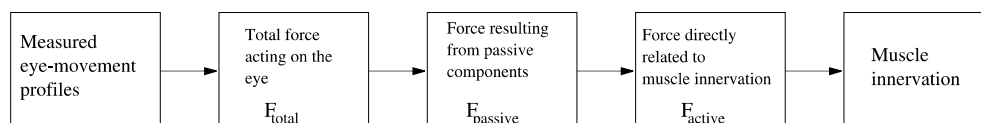

Fig. 2. Step-wise process of calculating muscle forces and innervation during saccades.

which include the muscle elasticity, orbital viscosity and orbital elasticity and which depends directly on eye orientation and velocity properties, were derived from the measured eye movement profiles using the eye plant model. To find the actively generated forces (F_{active}), which depend directly on the muscle innervation and which includes the contractile and viscous muscle properties, we subtracted $F_{passive}$ from F_{total}. We then used the eye plant model to find the innervation of the muscles that generated F_{active}.

2.1. Experimental procedures

The eye movements were recorded using the magnetic search coil technique (Collewijn, Van der Mark, & Jansen, 1975; Robinson, 1963). The movements of the right eye were sampled at 500 Hz and stored by a computer. The subject sat within the magnetic fields with his head immobilized with a bite bar. The five visual targets were back-projected onto a flat screen at the hight of the subjects eyes. The visual targets were Xs (24.5' of visual angle) and were constantly visible throughout the experiment. The subject was seated 1.5 m in front of the screen such that the right eye was aligned with the central target. The targets were positioned at 10° and 20° to the right and to the left of the central target. The subject made self paced saccades between each of these targets. Velocity profiles were computed by taking the first derivative of the measured eye position profiles. The eye movements between points of equal eccentricity were then pooled together to determine the mean eye movement profile (and standard deviation) for saccades between these two respective points. We also averaged over adducting and abducting eye movements in order to remove (average out) movement directional effects caused by inequalities between the lateral and medial rectus muscles. For the remainder of the work only the average movement profiles were used. The acceleration (α) profiles of these averaged eye movements were computed by taking the derivative of the velocity (ω) profiles ($\alpha = d\omega/dt$).

The total force acting on the eye was determined from the acceleration profiles by applying Newton's third law. The moment of inertia of the eye was assumed to be 4.3×10^{-5} gf s²/deg which is the average value for humans as reported by Clark and Stark (1974a).

The model of the eye plant that was used to simulate the forces acting on the eye is given in Section 2.2.

2.2. The eye plant model

The Hill-type mechanistic model of the horizontal saccadic system which is used in our work was based on similar models that were previously developed by Clark and Stark, 1974a,b; Collins et al. (1975a); Pfann et al. (1995) and Robinson and Zuber (1981). Most of the parameter values were derived from steady state measurements of macroscopic muscles properties (Collins, Carlson, Scorr, & Jampolsky, 1981; Collins et al., 1975b; Miller et al., 1999) and quick release experiments (Collins, Bach-Y-Rita, & Collins, 1971; Cook & Stark, 1967). The remaining parameter values were taken from the models by Robinson, Pfann and Clark (see Appendix A). The data presented in the above mentioned work was collected from measurements primarily in human strabismus patients (Collins et al., 1981; Robinson, O'Meara, Scott, & Collins, 1969), cats (Barmack, Bell, & Rence, 1971; Collins et al., 1971; Robinson, 1964) and monkeys (Fuchs & Lushei, 1971). Data was collected using non-invasive length–tension forceps (Collins et al., 1981) and chronically implanted muscle-force transducers (Collins et al., 1975b; Miller & Robins, 1992; Pfann et al., 1995). A diagram of the model is shown in Fig. 3.

The neural inputs (i.e. overall motoneuron activities) MN_{lr} and MN_{mr} are low pass filtered to generate the active internal muscle forces $F_{a_{lr}}$ and $F_{a_{mr}}$. In each muscle, the force generator is in parallel with a nonlinear dashpot, B, which represents the force–velocity relation of the active muscle. This unit is in series with an elastic element, K_{se}, which represents the connective tissue in series with contractile elements which has the experimentally measured property that an instantaneous reduction
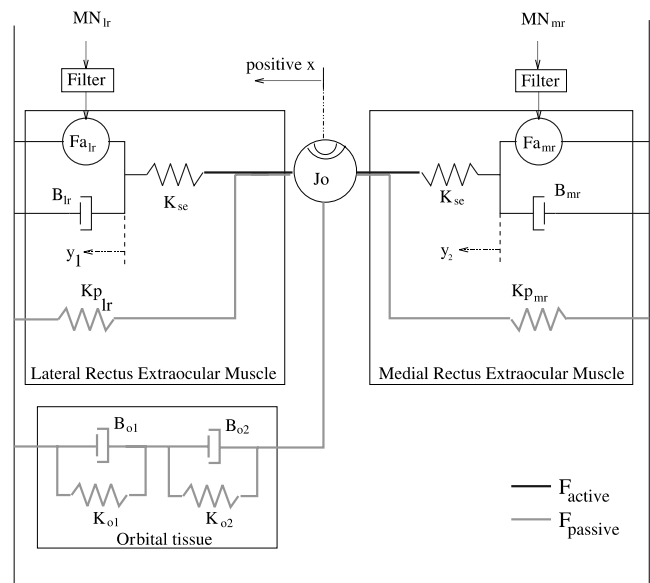

Fig. 3. Diagram of the model of the horizontal eye plant. The lateral and medial rectus muscle variables are denoted by subscripts lr and mr respectively. The input MN is the neural input converted to its force equivalent. The force generator F_a represents the length–tension–activation relationship of the muscles. The force–velocity relationship is provided by the viscosity B. The series-elastic element is denoted K_{se}. K_p represents the passive muscle elasticity. Orbital mechanics are modeled by a dual spring–dashpot system ($K_{o1}, B_{o1}, K_{o2}, B_{o2}$) together with the mass (J_o).

in load results in an instantaneous change in muscle length (i.e. the characteristics of a spring). This group of mechanical elements is in parallel with an elastic element, K_p, which represents the passive elastic properties of the muscle. Both F_a and K_p are non-linear. These muscle models are combined with a dual mass–spring–dashpot $(K_{o1}, B_{o1}, K_{o2}, B_{o2}, J_o)$ (Robinson, Bach-y-Rita, & Lennerstrand, 1975) representation of the orbit to model the horizontal saccadic system. Since the contribution of the vertical and oblique muscles to horizontal eye movements is negligible they have been lumped together with the model of the orbit. This simplification is of the same order of magnitude as the simplification that both horizontal muscles were taken to be of equal effective strength.

A more precise description of the model and the parameter values that were used is given in Appendix A.

3. Results

The eye movement measurements showed the same pattern of saccade duration, skewness and maximum speed differences between the centrifugal and centripetal saccades as reported by Collewijn et al. (1988) and Pelisson and Prablanc (1988). The average position and velocity profiles for the saccades between primary position (central target) and 20° eccentric are shown in Fig. 4. The results for the saccades between the primary position and 10° eccentric and between 10° and 20° eccentric showed the same characteristics and will therefore not be shown here.

$F_{passive}$, the force generated by the muscle elasticity (K_p) and the orbital tissue (B_o, K_o), depends only on eye orientation and velocity. The model of the eye plant therefore allowed us to compute $F_{passive}$ from the measured eye movement data as shown in Eq. (1)
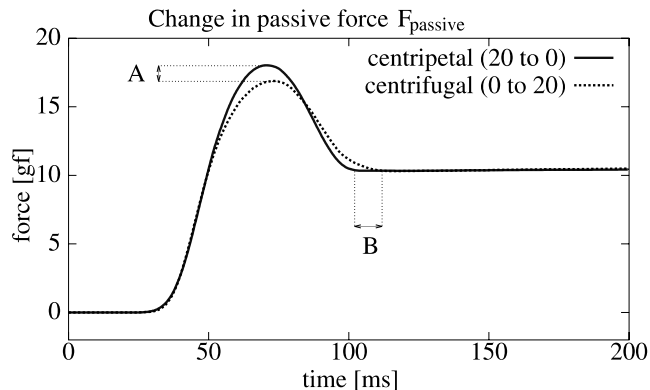

Fig. 5. Change in total passive force $F_{passive}$ during centripetal and centrifugal saccades between the central position and the target at 20° eccentricity. 'A' indicates the difference in maximum change in $F_{passive}$. 'B' indicates the difference in duration until steady state is reached.

$$F_{passive}(t) = F_{p_{lr}}(\theta(t)) - F_{p_{mr}}(\theta(t)) - F_o(\theta(t)), \quad (1)$$

where $F_{p_{lr}}$, $F_{p_{mr}}$ and F_o are the muscle elasticity and orbital tissue forces as defined in Appendix A. Fig. 5 shows the change in $F_{passive}$ during centripetal and centrifugal saccades. Fig. 6 shows the change in F_{active} during centripetal and centrifugal saccades which was found by subtracting $F_{passive}$ from F_{total}.

We show the change in force rather than the actual force since this makes it easier to compare the forces during centrifugal and centripetal saccades. No relevant information is lost by doing this since the steady state forces, i.e. the initial offset, of F_{active} and $F_{passive}$ cancel each other and therefore do not contribute to the generation of eye movements. The profiles of F_{active} and $F_{passive}$ look similar because, as we show in Section 3.1, the profile of $F_{passive}$ is a consequence of F_{active}. The muscle innervation that, according to our eye plant model, generates F_{active} is shown in Figs. 7 and 8. This muscle innervation was calculated by using a gradient
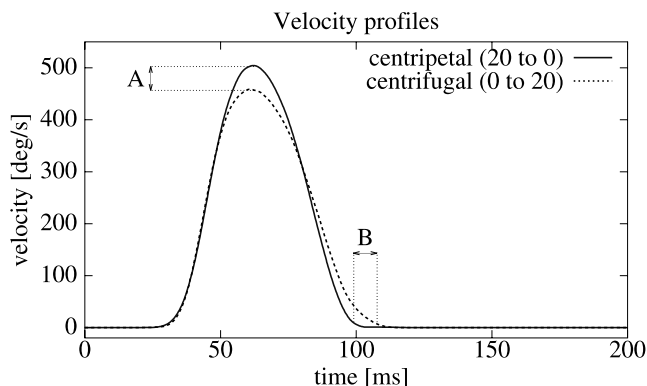

Fig. 4. Average velocity profiles for the centrifugal and centripetal saccades between the central position and the target at 20° eccentricity. The characteristic difference in maximum saccade velocity (A) and saccade duration (B) are indicated.
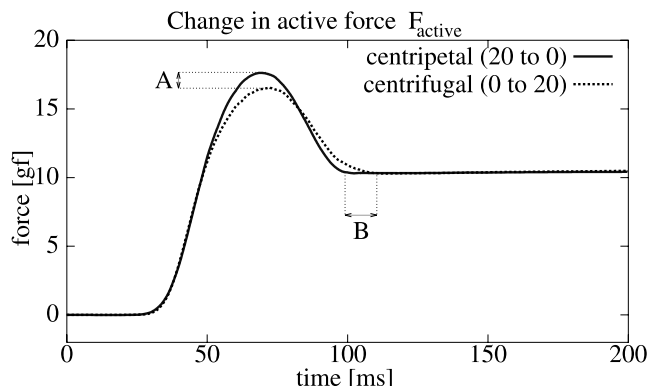

Fig. 6. Change in total active force F_{active} during centripetal and centrifugal saccades between the central position and the target at 20° eccentricity. 'A' indicates the difference in maximum change in F_{active}. 'B' indicates the difference in duration until steady state is reached.
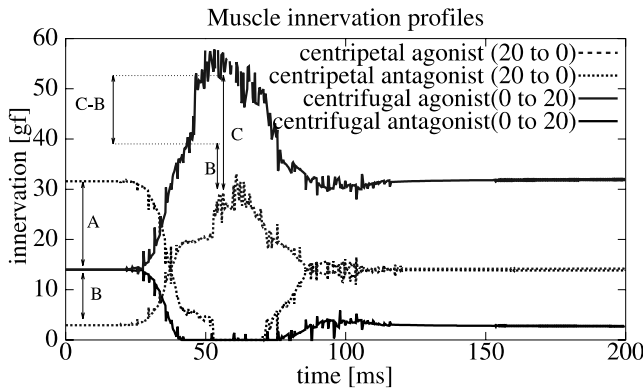
Fig. 7. Muscle innervation profiles showing the strength of agonist and antagonist activity during the saccade. 'A' indicates the difference in antagonist deactivation pulse amplitude between centripetal and centrifugal saccades. 'B' indicates the difference in initial agonist activity while 'C' indicates the difference in maximum agonist activity. 'C–B' therefore indicates the difference in agonist pulse amplitude between the centripetal and centrifugal saccades.
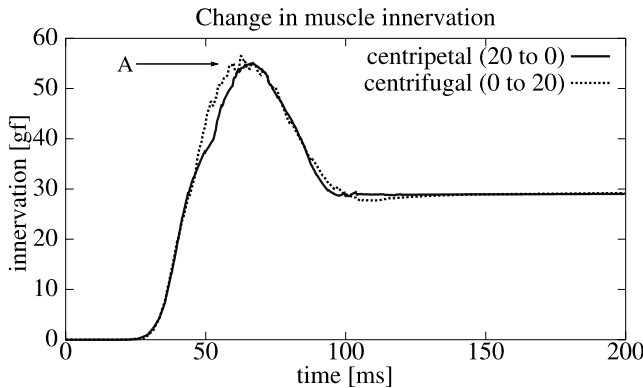

Fig. 8. Change in total neural muscle activity during centrifugal and centripetal saccades between the central position and the target at 20° eccentricity. 'A' indicates the (lack of) difference in maximum change in muscle activity.

descent search algorithm to find the innervations that would generate F_{active} when used as input to our eye plant model. The search space was reduced to a single dimension by the constraint that the activity change in antagonist is derived from the the activity change in the agonist via inhibitory inter-neurons in the brain stem (Cullen & Guitton, 1997; Hikosaka, Igusa, Nakao, & Shimazu, 1978; Igusa, Sasaki, & Shimazu, 1980; Robinson, Bach-y-Rita, et al., 1975; Scudder, 1988; Strassman, Highstein, & McCrea, 1986a,b; Yoshida, Berthoz, Vidal, & McCrea, 1982).

The muscle innervations calculated by us, and shown in Figs. 7 and 8, are given in grams of force (gf) rather than spikes per second because the force–length–innervation relationship (Miller et al., 1999; Collins et al., 1981; Miller & Robinson, 1984), which determines $F_{a_{lr}}$ and $F_{a_{mr}}$, gives muscle innervation in grams of force. The innervation of the muscles is defined as the isometric developed force (F_a) the muscle would generate if it were set at primary position length. This muscle innervation, although given in grams of force, is always directly related to the neural activity coming to the muscle.

3.1. Analysis of the $F_{passive}$ profiles

The force profiles in Fig. 5 reveal that $F_{passive}$ follows the same pattern as the velocity profiles for centrifugal and centripetal saccades. During centripetal saccades the passive-force profiles show a greater maximum change (Fig. 5'A') and a faster return to a steady state (Fig. 5'B') than during centrifugal saccades.

As we will now show, however, the direction in which the passive force pulls the eye is such that an increase in passive force corresponds to a reduction in the net-force driving the eye movement. Since the viscous force always acts opposite to the movement direction it is obvious that this component of the passive force should act to reduce movement velocity. The effect of the elastic forces however is less intuitive. The elastic forces pull the eye towards the central position, helping the eye movement during centripetal saccades and hindering the movement during centrifugal saccades. As the eye moves further away from the central position during centrifugal eye movements the passive elastic forces increase and counteract the centrifugal movement more strongly. As the eye moves closer to the central position during centripetal eye movements the strength of the elastic forces decreases, reducing its positive contribution to the eye movement. The change in passive force therefore acts to reduce the acceleration of the eye during centrifugal saccades as well as during centripetal saccades. Thus the greater maximum change in passive force during centripetal saccades as compared to centrifugal ones (Fig. 5) causes the passive force to slow down the centripetal saccade more then it does the centrifugal saccade.

If the difference in the forces $F_{passive}$ were the primary contribution to the difference in movement profiles during centripetal and centrifugal saccades, the centrifugal saccade would reach the greater maximum velocity. Since the velocity profiles show the reverse situation, i.e. a greater maximum velocity during centripetal saccades than during centrifugal ones, we must conclude that the cause of the observed difference in velocity profiles must lie somewhere in the active forces F_{active}.

Rather than being the cause of the difference in centrifugal and centripetal velocity profiles the difference in $F_{passive}$ during these eye movements is a consequence of the kinematic differences. The reason why $F_{passive}$ follows the eye movement profiles so linearly is because taken as a muscle pair the nonlinearities of the individual passive muscle elasticities cancel each other making $F_{passive}$ quasi-linear (Robinson et al., 1969). Since the orbital tissue forces included in $F_{passive}$, both the elasticity and

viscosity components, are also linear with respect to eye orientation the change in F_{passive} during an eye movement is independent of the starting orientation.

3.2. Analysis of the F_{active} profiles

The active force profiles in Fig. 6 illustrate the change in F_{active} during centrifugal and centripetal saccades. During centripetal saccades the active-force profiles shows a greater maximum change (Fig. 6'A') and return to a steady state faster (Fig. 6'B') than during centrifugal saccades. These characteristics are almost identical to those seen in the passive force profiles of Fig. 5. For the active force however the change in force contributes positively to the eye movement. The greater change in F_{active} during centripetal movements, as compared to the change in F_{active} during centrifugal movements, causes a greater acceleration of the eye. This, in combination with the previous results concerning F_{passive}, leads us to conclude that the cause of the velocity difference during centrifugal and centripetal saccades has to do with the properties of F_{active}. We now evaluate the contributions of the muscle innervation, the length–tension–innervation relation and the force–velocity relation of the muscles to the difference in F_{active} during centrifugal and centripetal saccades. By comparing these we will show that eventhough F_{active} is generated by the neural innervation of the muscles, the difference in F_{active} during centripetal and centrifugal saccades is due to mechanical influences on the generation of F_{active} and not due to differences between the neural signals.

3.2.1. Neural activity

The reduction in antagonist muscle deactivation step that Pelisson and Prablanc (1988) suggested as a possible cause of the kinematic differences between centrifugal and centripetal saccades can clearly be seen in the muscle innervation patterns shown in Fig. 7'A'. What the figure also shows however is that the pulse in agonist muscle innervation is greater during centrifugal saccades than during centripetal ones (7'C–B'). The reason for this increase in agonist innervation can be found in the non-linear relation between eye orientation and the required muscle activity to maintain fixation. Fig. 9 shows the muscle innervation values that were given by Miller et al. (1999) for fixation at various eye orientations. Due to this relationship between muscle innervation and eye orientation the agonist muscle must increase its activity more during a centrifugal eye movement (Fig. 9'A') than during a centripetal one (Fig. 9'B'), resulting in a greater agonist pulse. The reduction in antagonist deactivation step (Fig. 7'A') is therefore compensated by the increase in agonist pulse (Fig. 7'C–B'). The total effect of the reduction of the deactivation pulse in the antagonist and the increase in agonist activity can be seen in Fig. 8 which shows the change in total muscle innervation
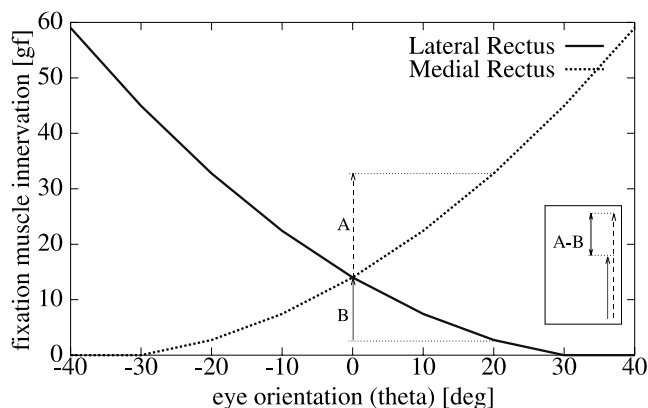

Fig. 9. Muscle innervation during fixation as a function of eye orientation for the two horizontal muscles, i.e. the medial and lateral rectus muscles. 'A' indicates the step in agonist muscle innervation increase during a centrifugal saccade of 20° away from the central position. 'B' indicates the step in agonist muscle innervation increase during a centripetal saccade of 20° towards the central position. The inset 'A–B' shows the difference between 'A' and 'B'. (Data from Miller et al., 1999.)

during centrifugal and centripetal saccades. Since the muscle-innervation-change profiles (Fig. 8) are almost identical for the centrifugal and centripetal saccades, the neural activity patterns cannot explain the observed velocity differences during centrifugal and centripetal saccades.

In order to show that this is not an artifact of our choice of eye plant model, Appendix B gives a more detailed analysis of the relation between the required change in steady-state muscle innervation (i.e. activity in the tonic neurons) and the muscle innervation change during a saccade.

3.2.2. Length–tension–innervation relation

The length–tension–innervation relation of the muscles was measured by Collins et al. (1975b), Miller et al. (1999), Robinson (1975) and is shown in Fig. 10. Depending on the degree of muscle stretch (i.e. the orientation of the eye) the force–innervation relation is altered as indicated by the different curves in Fig. 10. Due to the non-linearity of the force–innervation curves the same step in innervation change will result in different sized steps in force change depending on the initial eye orientation and muscle innervation (Fig. 10'B–A').

The effect of this length–tension–innervation relation on centripetal and centrifugal saccades (i.e. the contractile force changes) can be seen in Fig. 11, which shows the simulated change in total force generation (i.e. change in $F_{a_{\text{lr}}} - F_{a_{\text{mr}}}$ in Fig. 7) resulting from the muscle innervation profiles during centrifugal and centripetal saccades (Fig. 7). Even though there was no difference in the maximum change in total innervation (Fig. 7'A') between the centrifugal and centripetal saccades, there is
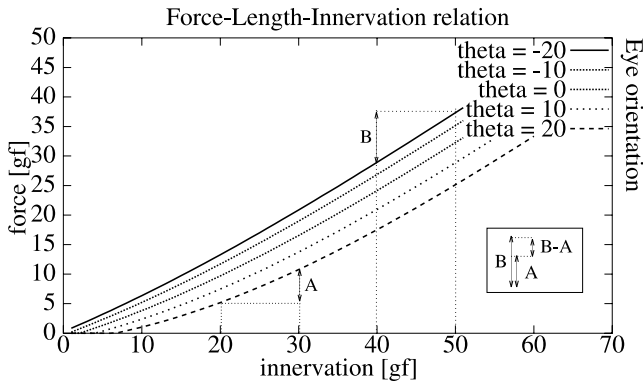
Fig. 10. Force–length–innervation curves showing the relationship between the contractile force generated by an extraocular muscle and its neural innervation for various degrees of muscle stretch (eye orientations). 'A' indicates the step in contractile muscle force resulting from a 10 gf increase of innervation when the eye is oriented 20° rightward with an initial activity level of 20 gf. 'B' indicates the step in contractile muscle force resulting from a 10 gf increase in muscle innervation when the eye is oriented 20° leftward with an initial innervation level of 40 gf. The inset 'B–A' indicates the difference between 'A' and 'B'. (Data from Miller et al., 1999.)
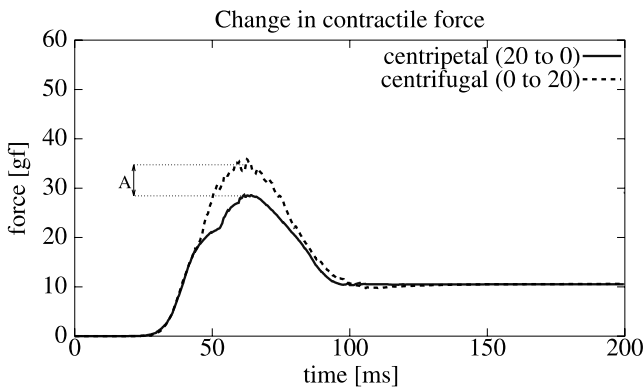

Fig. 11. Change in total contractile force (and muscle innervation) during centripetal and centrifugal saccades between the central position and the target at 20° eccentricity. 'A' indicates the difference in maximum change in generated contractile force.

a clearly discernable difference in the resulting maximum change in contractile force (Fig. 11'A').

The length–tension–innervation relation results in a larger maximum change in contractile force during centrifugal saccades than during centripetal ones (Fig. 11'A'). This is contrary to the difference in F_{active} where we found that the maximum change in F_{active} is greater for centripetal than for centrifugal saccades (Fig. 6'A'). The cause of the difference in F_{active} and thus the cause of the kinematic differences during centripetal and centrifugal saccades, therefore, can not be in the length–tension–innervation relationship of the muscles.

3.2.3. Force–velocity relation

The force–velocity relationship of the muscles (B_{lr} and B_{mr} in Fig. 3) describes the viscous force generated

in the muscles as a function of the rate of muscle shortening (lengthening).

The muscle viscosity relationship that was derived by Hilll (1938) and which was also used in the models by Clark and Stark (1974a,b), Cook and Stark, 1967 and Pfann et al. (1995) is as follows:

$$F_{viscous} = B\frac{dy}{dt}, \quad \text{where}$$

$$B = \begin{cases} \dfrac{3F_a}{H_{v_{max}}}, & \text{when the muscle expands} \\ \dfrac{1.25F_a}{H_{v_{max}} + \dfrac{dy}{dv}}, & \text{when the muscle contracts} \end{cases} \quad (2)$$

where $H_{v_{max}} = 900$ deg/s is the Hill constant characterizing the relationship to the maximum rate of muscle shortening, F_a is the contractile force of the muscle and dy/dt is the rate of muscle shortening (lengthening).

The viscous forces in both muscles act against the movement direction. Thus the net viscous force acting on the system is the sum of the viscous forces. This is an important difference between the viscous forces and the elastic and contractile forces, which act in opposite directions in both muscles. The net viscosity coefficient B is therefore a function of $F_{a_{lr}} + F_{a_{mr}}$ (Fig. 12). In addition, the viscous force is a function of the contraction rate (dy/dt). The value of the viscosity coefficient B is therefore only of importance during the actual saccade (period 'A' in Fig. 12).

When we simulate the viscous forces in the muscles using Eq. (2), we find that the net viscous forces during centrifugal saccades reach a much greater maximum force then during centripetal saccades (Fig. 13'A'). Subtracting the viscous force, which acts to slow down the eye movement, from the contractile muscle force results in the net muscle force profiles shown in Fig. 14. During centripetal saccades the resulting force profiles (Fig. 14) show a greater maximum change (Fig. 14'A') and return
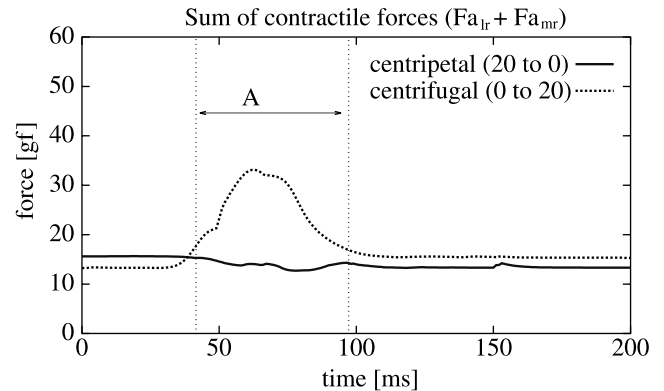

Fig. 12. Sum of contractile forces $F_{a_{lr}}$ and $F_{a_{mr}}$ during centrifugal and centripetal saccades between the central position and the target at 20° eccentricity. 'A' indicates the period during which the muscle contraction rate dy/dt is most significant.
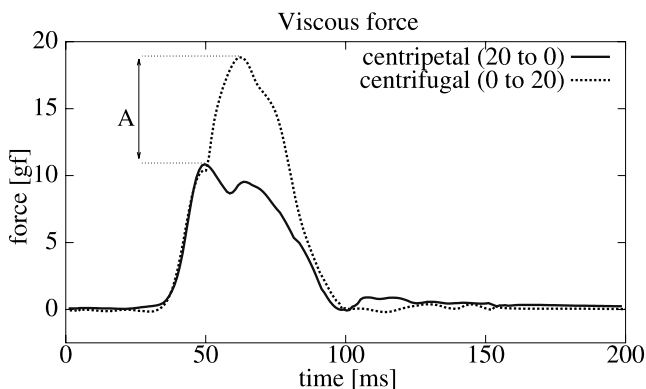
Viscous force

Fig. 13. Total viscous force during centripetal and centrifugal saccades between the central position and the target at 20° eccentricity. 'A' indicates the difference in maximum viscous force.
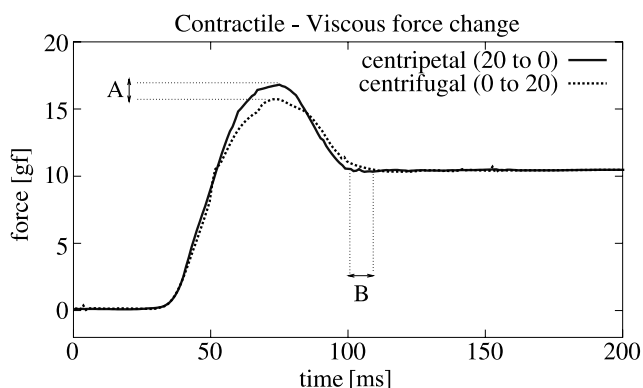
Contractile - Viscous force change

Fig. 14. The result of subtracting the total viscous muscle force from the total change in contractile muscle force during centripetal and centrifugal saccades between the central position and the target at 20° eccentricity. 'A' indicates the difference in maximum change in the resulting force. 'B' indicates the difference in duration until steady state is reached.

to steady state faster (Fig. 14'B') than during centrifugal saccades. This agrees with the maximum velocity and duration characteristics of centripetal and centrifugal saccades. We therefore conclude that the cause of the kinematic differences between centrifugal and centripetal saccades is in the muscle viscosity.

4. Discussion

The intention of the present study was to determine the cause of the kinematic differences between saccades going away from the primary position and saccades going towards the primary position. In other words, what causes centrifugal saccades to have a lower maximum velocity and a longer duration than centripetal saccades?

We measured the eye movements during centrifugal and centripetal saccades and used a model of the eye plant to simulate the muscle and orbital tissue forces

acting on the eye during these saccades. Using the resulting force profiles and the data on muscle properties from experiments by Collins et al. (1975a,b), Miller and Robinson (1984), Miller et al. (1999), Robinson (1975), and Robinson and Zuber (1981), we showed that the contribution of the passive forces (i.e. the muscle elasticity and orbital tissue elasticity and viscosity) to the kinematics of centrifugal and centripetal saccades differs only as a result of the difference in movement profiles. In addition, we showed that the contribution of the passive forces to the ocular kinematics favors the centrifugal saccades. From this we concluded that the passive forces can not be the cause of the kinematic differences.

Next we investigated the active forces, i.e. the muscle contractile force and the muscle viscosity, which both depend directly on the innervation of the muscles. By synthesizing the muscle innervation that would be required to produce the active forces we showed that the total change in muscle innervation during centrifugal and centripetal saccades is near identical and can therefore not be the cause of the kinematic differences. Based on the length–tension–innervation relationship of the eye muscles that was reported by Miller et al. (1999) and Robinson (1975) we showed that the contractile forces resulting from the innervation change are greater during centrifugal saccades than during centripetal ones. The contractile length–tension–innervation relationship can therefore not be the cause of the observed kinematic differences either. The muscle viscosity was investigated next. We found that, due to the non-linear characteristics of the muscle viscosity as described by Clark and Stark (1974a,b), Cook and Stark (1967), Hilll (1938) and Pfann et al. (1995) the viscous force is much greater during centrifugal movements than during centripetal ones. This means that the muscle viscosity slows down the eye movement more during centrifugal movements resulting in a lower maximum velocity.

The muscle viscosity was the only force that showed a difference between centrifugal and centripetal saccades which could explain the observed difference in saccade kinematics. We therefore conclude that the cause of the kinematic differences during centrifugal and centripetal saccades is the non-linear force–velocity relationship of the muscles.

4.1. Implications for the saccade generator

It is generally accepted that during saccades the only feedback signal available to the system is some kind of efference copy signal which either encodes eye orientation (Robinson, Bach-y-Rita, et al., 1975) or eye displacement (Jurgens, Becker, & Kornhuber, 1981). Any deviations in the eye movements that are not reflected in the muscle innervation, such as mechanical defects, can therefore only be detected if they effect the amplitude

and/or duration of the saccade. The result of our current investigation is that the difference between centrifugal and centripetal saccades has its cause in the mechanics of the eye plant, specifically the muscle viscosity. The difference in saccade kinematics is not reflected in the neural feedback signal. Since the amplitude of the saccades is not effected either the only way that the saccadic system could measure these kinematic differences is if the centrifugal saccade is sufficiently slow so that the difference in duration interferes with the functioning of the visual system. From the data by Collewijn et al. (1988), the difference in saccade duration for saccades of up to 30° is less than 25 ms. Considering that the minimal inter-saccadic interval during rapid search is approximately 135 ms (Becker & Juergens, 1979) it is improbable that a difference in saccade duration of (less than) 25 ms is noticeable. We therefore conclude that the saccadic system is unable to detect the kinematic differences between centrifugal and centripetal saccades.

4.2. Implications for starting position dependent modulation

In Section 3.2 and Appendix B we showed that regardless of the lower bound cutoff of the antagonist signal the total change in muscle innervation during centrifugal and centripetal saccades is nearly identical. The reason why centrifugal and centripetal saccades have the same pattern in total change in muscle innervation is because the difference in antagonist signal cutoff is compensated by the position dependent increase in agonist signal for centrifugal saccades. According to the more recent models of the saccade generator (Quaia et al., 1999), the superior colliculus generates a saccade drive signal, based on the desired displacement of the eye, and this signal is then modulated by a signal from the cerebellum to compensate for position-dependent differences. The difference in agonist pulse activity (which compensates the cutoff effect) would thus have to be the results of the modulation signal from the cerebellum. Using the same method as we did (see Appendix B) to find the difference in agonist pulse activity during centripetal and centrifugal saccades may therefore provide a useful tool to quantify the modulation signal sent by the cerebellum.

4.3. Conclusion

By using the results of force measurements that were made in recent years (Miller et al., 1999) we were able to simulate the muscle forces during centrifugal and centripetal saccades. Using this simulation we found that the cause of the kinematic differences between centrifugal and centripetal saccades is in the muscle viscosity.

Appendix A. The eye plant model

This appendix describes the implementation of the eye plant model.

As shown in Fig. 3 the model of the eye plant consists of three distinct parts, the passive orbital tissue (including the moment of inertia of the eye ball) and the two horizontal extraocular muscles. For simplicity the models of the lateral and medial rectus muscles are identical. The four percent difference in muscle strength between the lateral and medial rectus muscles which is reported by Miller et al. (1999) was not included in our model.

The moment of inertia of the orbit was taken from (Clark & Stark, 1974a) giving a value of $J = 4.3e - 5$, gf s^2/deg. The orbital tissue force parameters were chosen such that the stead-state muscle forces given in Miller et al. (1999) would result in fixation (this determines K_o) while the time constants (τ_1, τ_2 and τ_3) were chosen as an average of the values given by other authors (Robinson & Zuber, 1981; Collins et al., 1981; Clark & Stark, 1974b). The orbital tissue force is given by the following equation:

$$F_o(\theta(t)) = K_o \left(\theta(t) + (\tau_1 + \tau_2)\frac{d\theta(t)}{dt} + \tau_1\tau_2\frac{d^2\theta(t)}{dt^2} \right) - \tau_3\frac{dF_o(\theta(t))}{dt}$$

where $\tau_1 = B_{o1}/K_{o1} = 50$ ms, $\tau_2 = B_{o2}/K_{o2} = 140$ ms, $\tau_3 = (B_{o1} + B_{o2})/(K_{o1} + K_{o2}) = 80$ ms and $K_o = (K_{o1} K_{o2})/(K_{o1} + K_{o2}) = 0.27$ gf/deg.

The passive elastic force of the muscles was determined by fitting the data presented in (Miller et al., 1999). For the lateral and medial rectus muscles this works out to:

$$F_{p_{lr}}(\theta(t)) = 0.002(\max(0, -\theta(t) + 35))^2,$$
$$F_{p_{mr}}(\theta(t)) = 0.002(\max(0, \theta(t) + 35))^2.$$

For the series elastic stiffness we took the average of the values given in Clark and Stark (1974a), Collins et al. (1975a), Pfann et al. (1995) and Robinson and Zuber (1981) resulting in $K_{se} = 2$ gf/deg. The muscle activation and deactivation time constants τ_a and τ_d, which determine the low-pass filter characteristic between the motoneuron activity and the muscle contraction, were taken from (Clark & Stark, 1974b; Pfann et al., 1995) as 4 and 8 ms respectively. The change in muscle activity (I) as function of the motoneuron activity is given by:

$$\frac{dI(t)}{dt} = \frac{1}{\tau_{a/d}}(I(t) - MN(t))$$

The active contractile force generated by the muscles was determined using a polynomial approximation ($F_a(\theta, I) = a\delta l + bI + cI\delta l \ldots$, where δl is the percentage

change in muscle length in relation to its relaxed length) of the length–tension–innervation data provided by (Miller et al., 1999) (Fig. 10). For the lateral rectus muscle $\delta l_{lr}(\theta) = -(53.5/80)\theta + 13.25$, for the medial rectus muscle $\delta l_{mr}(\theta) = (53.5/80)\theta + 13.25$.

The muscle viscosities (B_{lr} and B_{mr}) determining the force–velocity relationship were based on the model presented in (Pfann et al., 1995) and look as follows:

$$B_{lr} = \begin{cases} \dfrac{3F_{a_{lr}}}{H_{v_{max}}}, & \text{if } \dfrac{dy_1}{dt} < 0 \\[2ex] \dfrac{1.25F_{a_{lr}}}{H_{v_{max}} + \dfrac{dy_1}{dt}}, & \text{otherwise} \end{cases}$$

$$B_{mr} = \begin{cases} \dfrac{3F_{a_{mr}}}{H_{v_{max}}}, & \text{if } \dfrac{dy_2}{dt} > 0 \\[2ex] \dfrac{1.25F_{a_{mr}}}{H_{v_{max}} - \dfrac{dy_2}{dt}}, & \text{otherwise} \end{cases}$$

where $H_{v_{max}} = 900$ deg/s is the Hill constant characterizing the relationship to the maximum rate of muscle shortening.

Using these model parameters the relationship of eye movement to muscle innervation is given by the following differential equations:

$$\frac{d\omega}{dt} = \frac{1}{J}(-F_o(\theta(t)) + F_{p_{lr}}(\theta(t)) + K_{se}(y_1(t) - \theta(t))$$
$$- F_{p_{mr}}(\theta(t)) - K_{se}(\theta(t) - y_2(t)))$$

$$\frac{dy_1}{dt} = \frac{F_{a_{lr}} + K_{se}(\theta(t) - y_1(t))}{B_{lr}},$$

$$\frac{dy_2}{dt} = \frac{-F_{a_{mr}} + K_{se}(\theta(t) - y_2(t))}{B_{mr}}$$

Appendix B. Neural activity profiles during saccades

The motoneuron activity (MN), i.e. muscle innervation, is generally assumed to be the sum of the tonic neuron activity (TN) and the burst neuron activity (excitatory EBN for agonist, inhibitory IBN for antagonist) (Gancarz & Grossberg, 1998; Robinson, Bach-y-Rita, et al., 1975; Scudder, 1988).

$$MN_{agonist} = TN_{agonist} + EBN_{agonist}, \quad \text{and}$$

$$MN_{antagonist} = \max(0, TN_{antagonist} - IBN_{antagonist}), \quad \text{with}$$

$$TN_{agonist}(T) = TN_{agonist}(0) + \alpha \int_0^T EBN_{agonist}(t)\,dt,$$

$$TN_{antagonist}(T) = TN_{antagonist}(0) - \beta \int_0^T IBN_{antagonist}(t)\,dt,$$

where α and β are synaptic gain factors and T is the duration of the saccade.

Tonic neuron activities at the beginning and end of saccades (i.e. the steady-state values) are known from the data by Miller et al. (1999, Fig. 9). Assuming that the shape of the burst neuron activity profile is the same for centrifugal and centripetal saccades, i.e. any difference in motoneuron activity is the result of the lower-bound cutoff effect described by Pelisson and Prablanc (1988) (see Section 1), the only free parameters that are left are α and β. Different values of α and β result in different MN profile shapes, altering the hight of the pulse part in the pulse-step profile. The values that we chose for our main work were chosen to give a pulse-step profile whose shape corresponds to the data reported by Collins et al. (1975a), Cullen and Guitton (1997), Robinson, Bach-y-Rita, et al. (1975) and Robinson (1975). To test the effect of different α and β values we varied α and β from 4 to 32 in steps of 4. Values of α larger than 32 cause the MN profiles to loose the pulse-step shape reported in the literature (Collins et al., 1975a; Cullen & Guitton, 1997; Robinson, Bach-y-Rita, et al., 1975). The values we used in the main text were $\alpha = 16$ and $\beta = 16$.

The maximum change in total activity during the centripetal saccade became larger than the maximum change in activity during centrifugal saccade when $\alpha > 16$ and $\beta < 16$. This difference was greatest when the gain factors $\alpha = 4$, $\beta = 32$ were chosen. When $\alpha < 16$ and $\beta > 16$ the maximum change in activity was larger during the centrifugal saccade then during the centripetal saccade. This difference was greatest when the gain factors $\alpha = 32$, $\beta = 4$ were chosen. Fig. 15 shows the total change muscle innervation profiles during centripetal and centrifugal saccades for these α, β pairs for saccades between the central target and a target at 20° eccentricity.

In order to see if the greater maximum change in muscle innervation during the centripetal saccade that was achieved when $\alpha = 32$ and $\beta = 4$ could explain the
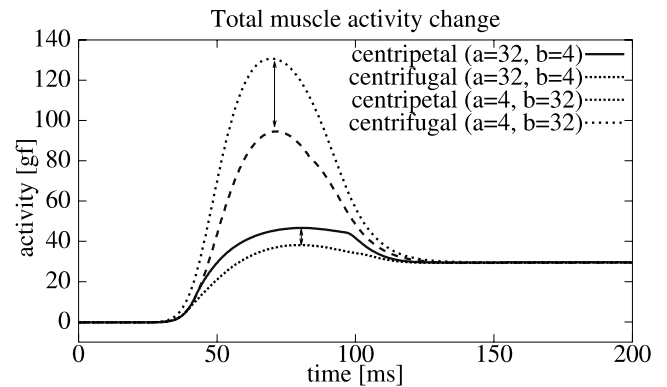

Fig. 15. Total change in muscle innervation during centripetal and centrifugal saccades between the central target and a target at 20° eccentricity. The arrows indicate the maximum difference in total muscle innervation change for each pair of $\alpha(a)$ and $\beta(b)$ values.
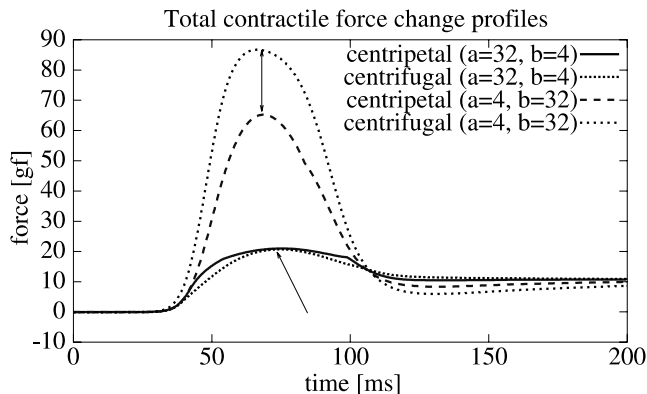
Fig. 16. Total change in generated contractile force in the muscles during centripetal and centrifugal saccades between targets at the central position and 20° eccentric.

difference in velocity profiles during centripetal and centrifugal saccades we also simulated the contractile muscle forces that would result from these muscle innervation profiles.

As we can see from Fig. 10 the non-linear force–length–activity relation (Fig. 10) of the muscles, which favors the centrifugal eye movement (Section 3.2), has resulted in total contractile muscle force changes with the same maximum value for both the centripetal and centrifugal eye movements (Fig. 16 $a = 32$, $b = 4$).

References

Abel, A., Dell'Osso, L. F., Daroff, R. B., & Parker, L. (1979). Saccades in extremes of lateral gaze. *Investigative Ophthalmology and Visual Science, 18*, 324–327.

Barmack, N. H., Bell, C. C., & Rence, B. G. (1971). Tension and rate of tension development during isometric responses of extraocular muscles. *Journal of Neurophysiology, 34*, 1072–1079.

Becker, W., & Juergens, R. (1979). An analysis of the saccadic system by means of double step stimuli. *Vision Research, 19*, 967–983.

Clark, M. R., & Stark, L. (1974a). Control of human eye movements: I. Modeling of extraocular muscle. *Mathematical Biosciences, 20*, 191–211.

Clark, M. R., & Stark, L. (1974b). Control of human eye movements: II. A model for the extraocular plant mechanism. *Mathematical Biosciences, 20*, 213–238.

Collewijn, H., Erkelens, C. J., & Steinman, R. M. (1988). Binocular coordination of human horizontal saccadic eye movements. *Journal of Physiology, 404*, 157–182.

Collewijn, H., Van der Mark, F., & Jansen, T. C. (1975). Precise recording of human eye movements. *Vision Research, 15*, 447–450.

Collins, C. C., Bach-Y-Rita, P., & Collins, C. C. (Eds.). (1971). *The control of eye movements* (pp. 283–325). New York: Academic Press.

Collins, C. C., Carlson, M. R., Scorr, A. B., & Jampolsky, A. (1981). Extraocular muscle forces in normal human subjects. *Investigative Ophthalmology and Visual Science, 20*, 652–664.

Collins, C. C., Lennerstrand, G., & Bach-Y-Rita, P. (Eds.). (1975a). *Proceedings of the international symposium, Wenner-Gren Center, Stockholm, June 4–6, Basic mechanisms of ocular motility and their clinical implications* (pp. 145–180). Oxford: Pergamon Press.

Collins, C. C., O'Meara, D., & Scott, A. B. (1975b). Muscle tension during unrestrained human eye movements. *Journal of Physiology, 245*, 351–369.

Cook, G., & Stark, L. (1967). Derivation of a model for the human eye-positioning mechanism. *Bulletin of Mathematical Biophysics, 29*, 153.

Cook, G., & Stark, L. (1968). The human eye movement mechanism. Experiments, modeling, and model testing. *Archives of Ophthalmology, 79*, 428–436.

Cullen, C. A., & Guitton, D. (1997). Analysis of Primate IBN Spike Trains Using System identification techniques. I. Relationship to eye movement dynamics during head-fixed saccades. *Journal of Neurophysiology, 78*, 3259–3282.

Eggert, T., Mezger, F., Robinson, F., Straube, A. (1999). Orbital position dependency is different for the gain of externally and internally triggered saccades. *NeuroReport, 10*, 2665–2670.

Fuchs, A. F., & Lushei, E. S. (1970). Firing patterns of abducens neurons of alert monkeys in relationship to horizontal eye movements. *Journal of Neurophysiology, 33*, 382–392.

Fuchs, A. F., & Lushei, E. S. (1971). Development of isometric tension in simian extraocular muscle. *Journal of Physiology, 219*, 155–166.

Fuchs, A. F., Kaneko, C. R. S., & Scudder, C. A. (1985). Brainstem control of saccadic eye movements. *Annual Review of Neuroscience, 8*, 307–337.

Gancarz, G., & Grossberg, S. (1998). A neural model of the saccade generator in the reticular formation. *Neural Networks, 11*, 1159–1174.

Hikosaka, O., Igusa, Y., Nakao, S., & Shimazu, H. (1978). Direct inhibitory synaptic linkage of pontomedullary reticular burst neurons with abducens motoneurons in the cat. *Experimental Brain Research, 33*, 337–352.

Hilll, A. V. (1938). The heat of shortening and the dynamic constants of muscle. *Proceedings of Royal Society, 126B*, 136–195.

Igusa, Y., Sasaki, S., & Shimazu, H. (1980). Excitatory premotor burst neurons in the cat pontine reticular formation related to the quick phase of vestibular nystagmus. *Brain Research, 182*, 451–456.

Jurgens, R., Becker, W., & Kornhuber, H. (1981). Natural and drug-induced variation of velocity and duration of human saccadic eye movements: evidence for control of the neural pulse generator by local feedback. *Biological Cybernetics, 39*, 87–96.

Miller, J. M., Pavlovski, D. S., & Shamaeva, I. (1999). *Orbit™ 1.8 Gaze mechanics simulation*. San Francisco: Eidactics.

Miller, J. M., & Robins, D. (1992). Extraocular muscle forces in alert monkey. *Vision Research, 32*, 1099–1113.

Miller, J. M., & Robinson, D. A. (1984). A model of the mechanics of binocular alignment. *Computers and Biomedical Research, 17*, 436–470.

Pelisson, D., & Prablanc, C. (1988). Kinematics of centrifugal and centripetal saccadic eye movements in man. *Vision Research, 28*, 87–94.

Pfann, K. D., Keller, E. L., & Miller, J. M. (1995). New models of the oculomotor mechanics based on data obtained with chronic muscle force transducers. *Annals of Biomedical Engineering, 23*, 346–358.

Quaia, C., Lefevre, P., & Optican, L. M. (1999). Model of the control of saccades by superior colliculus and cerebellum. *Journal of Neurophysiology, 82*, 999–1018.

Robinson, D. A. (1963). A method of measuring eye movements using a search coil in a magnetic field. *IEEE Transactions of Biomedical Engineering, 10*, 137–145.

Robinson, D. A. (1964). The mechanisms of human saccadic eye movement. *Journal of Physiology—London, 174*, 245–264.

Robinson, D. A. (1970). Oculomotor unit behavior in the monkey. *Journal of Neurophysiology, 33*, 393–404.

Robinson, D. A. (1975). A quantitative analysis of extraocular muscle cooperation and squint. *Investigative Ophthalmology, 14*, 801–825.

Robinson, D. A., Bach-y-Rita, P., & Lennerstrand, G. (Eds.). (1975). *Basic mechanisms of ocular motility and their clinical implication*. Oxford: Pergamon.

Robinson, D. A., O'Meara, D. M., Scott, A. B., & Collins, C. C. (1969). Mechanical components of human eye movements. *Journal of Applied Physiology, 26*, 548–553.

Robinson, D. A., & Zuber, B. L. (Eds.). (1981). *Models of oculomotor behavior and control* (pp. 21–42). Boca Raton: CRC Press.

Rottach, K. G., Das, V. E., Wohlgemuth, W., Zivotofsky, A. Z., & Leigh, R. J. (1998). Properties of horizontal saccades accompanied by blink. *Journal of Neurophysiology, 79*, 2895–2902.

Scudder, C. A. (1988). A new local feedback model of the saccadic burst generator. *Journal of Neurophysiology, 59*, 1455–1475.

Strassman, A., Highstein, S. M., & McCrea, R. A. (1986a). Anatomy and physiology of saccadic burst neurons in the alert squirrel monkey. I. Excitatory burst neurons. *Journal of Comparative Neurology, 249*, 337–357.

Strassman, A., Highstein, S. M., & McCrea, R. A. (1986b). Anatomy and physiology of saccadic burst neurons in the alert squirrel monkey. II. Inhibitory burst neurons. *Journal of Comparative Neurology, 249*, 358–380.

Yoshida, K., Berthoz, A., Vidal, P. P., & McCrea, R. A. (1982). Morphological and physiological characteristics of inhibitory burst neurons controlling rapid eye movements on the alert cat. *Journal of Neurophysiology, 48*, 761–784.